2-Cyanopropan-2-yl versus 1-Cyanocyclohex-1-yl Leaving Group: Comparing Reactivities of Symmetrical Trithiocarbonates in RAFT Polymerization

Oleksandr Ivanchenko, Maksym Odnoroh, Faustine Rolle, Asja Kroeger, Sonia Mallet-Ladeira, Stéphane Mazières, Marc Guerre, Michelle Coote, Mathias Destarac

Macromolecular Rapid Communications
www.mrc-journal.de

2-Cyanopropan-2-yl versus 1-Cyanocyclohex-1-yl Leaving Group: Comparing Reactivities of Symmetrical Trithiocarbonates in RAFT Polymerization

*Oleksandr Ivanchenko, Maksym Odnoroh, Faustine Rolle, Asja A. Kroeger, Sonia Mallet-Ladeira, Stéphane Mazières, Marc Guerre, Michelle L. Coote, and Mathias Destarac**

This study introduces bis(1-cyanocyclohex-1-yl)trithiocarbonate (TTC-bCCH) as a novel trithiocarbonate chain transfer agent and compares its reactivity with the previously described bis(2-cyanopropan-2-yl)trithiocarbonate (TTC-bCP) for the reversible addition-fragmentation chain transfer (RAFT) polymerization of styrene (St), *n*-butyl acrylate (*n*BA), and methyl methacrylate (MMA). Significant findings include the effective control of M_n and low dispersities from the onset of polymerization of St and *n*BA showing swift addition-fragmentation kinetics, leading to similar behaviors between the two RAFT agents. In contrast, a fourfold decrease of the chain transfer constant to MMA is established for TTC-bCCH over TTC-bCP. This trend is confirmed through density functional theory (DFT) calculations. Finally, the study compares thermoplastic elastomer properties of all-(meth)acrylic ABA block copolymers produced with both RAFT agents. The impact of dispersity of PMMA blocks on thermomechanical properties evaluated via rheological analysis reveals a more pronounced temperature dependence of the storage modulus (G') for the triblock copolymer synthesized with TTC-bCCH, indicating potential alteration of the phase separation.

1. Introduction

Trithiocarbonates (TTCs) find extensive use as chain transfer agents in reversible addition-fragmentation chain transfer (RAFT) polymerization.[1,2] This is attributed to their high efficiency in producing well-defined macromolecular structures from a large selection of monomers including styrene and derivatives, acrylamides, acrylates, and methacrylates.[2] Trithiocarbonates can be categorized into two distinct groups: unsymmetrical (e.g., R′ = *n*-alkyl, **Scheme 1a**) and symmetrical TTCs. Both unsymmetrical and symmetrical trithiocarbonates exhibit effective control over the polymerization of the aforementioned monomers, provided that the leaving group R is carefully chosen.[2] In particular for methacrylates, only electron-withdrawing and mostly cyano-containing tertiary leaving groups (e.g., 2-cyanopropan-2-yl, Scheme 1b)[2] give good control of molar mass and dispersity.[1]

So far unsymmetrical TTCs are widely used for classical diblock and multiblock synthesis. Many of them have been tested in RAFT polymerization with some being commercially available in small quantities and few of them potentially supplied at the industrial scale.[3,4] Conversely, symmetrical TTCs, although less explored, hold their own unique domain of significance. They mainly serve as precursors for ABA triblock copolymers through a two-step convergent synthesis procedure.[1]

Well-designed ABA-type block copolymers demonstrate remarkable capabilities when they consist of a thermodynamically immiscible soft mid-block B (with a glass transition temperature (T_g) below ambient temperature) and rigid outer blocks A (amorphous or semicrystalline). In this configuration, the ABA copolymer spontaneously assembles itself at the nanoscale into diverse morphologies, resulting in intermolecular physical crosslinks within the rigid domains. The distinctive behavior exhibited by such ABA-type copolymers imparts them with thermoplastic elastomer (TPE) properties.[5] TPEs offer rubber-like characteristics during use combined with the advantageous processability and recyclability inherent to thermoplastics. Consequently, in the ongoing pursuit of increasingly sustainable polymer solutions,

O. Ivanchenko, M. Odnoroh, F. Rolle, S. Mazières, M. Guerre, M. Destarac
Laboratoire SOFTMAT
Université Toulouse 3 – Paul Sabatier
CNRS UMR 5623
118 route de Narbonne, Toulouse 31062, France
E-mail: mathias.destarac@univ-tlse3.fr
A. A. Kroeger, M. L. Coote
Institute for Nanoscale Science & Technology
Flinders University
Adelaide, South Australia 5042, Australia
S. Mallet-Ladeira
Institut de Chimie de Toulouse (UAR 2599) / Université Toulouse 3 – Paul Sabatier
118 route de Narbonne, Toulouse 31062, France
The ORCID identification number(s) for the author(s) of this article can be found under https://doi.org/10.1002/marc.202400317

DOI: 10.1002/marc.202400317

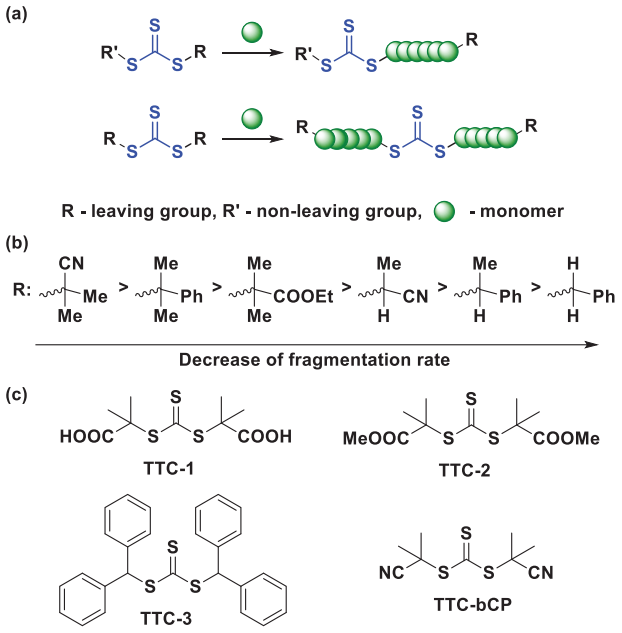

Scheme 1. a) Polymerization of vinyl monomers using either unsymmetrical or symmetrical TTC. b) Most common leaving groups of RAFT agents and symmetrical TTCs investigated in methacrylate polymerization.

ABA triblock copolymers largely contribute to the TPEs market growth.[6] These copolymers find wide-ranging applications including elastomers, pressure-sensitive adhesives, coatings, and toughening agents, among other uses.[5] For instance, styrenic block copolymers, such as polystyrene–polybutadiene–polystyrene (SBS), constitute a widely utilized category of TPEs. However, SBS copolymers present certain limitations, including a restricted upper service temperature due to the low T_g (around 100 °C) of the polystyrene hard domains. Additionally, their susceptibility to UV and oxidation is attributed to the unsaturated nature of the copolymer. An alternative to SBS is provided by all-(meth)acrylic TPEs (e.g., methacrylate-acrylate-methacrylate), which present several advantages. These include superior optical transparency, enhanced weather resistance, inherent tackiness, and low viscosity.[4,7] On an industrial scale, all-(meth)acrylic TPEs were developed by Kuraray through living anionic polymerization[8] and by Arkema via nitroxide-mediated reversible-deactivation radical polymerization (NMP).[4,9]

In the pursuit of achieving all-(meth)acrylic ABA copolymers with low dispersity, the RAFT polymerization method encounters a challenge due to the scarcity of symmetrical TTCs that possess appropriate tertiary leaving groups for achieving optimal control over methacrylate polymerization.[10–13] There have been several attempts to synthesize PMMA from different symmetrical TTCs. For instance TTC bearing 2-carboxypropan-2-yl group (**TTC-1**, Scheme 1c)[11–13] did not lead to well-defined methacrylic blocks ($Đ$ = 1.4–1.8) and no control over molar mass was observed. The ester analogue of this TTC (**TTC-2**, Scheme 1c)[10] also did not show an efficient control of the polymerization of MMA with a chain transfer constant $C_{tr} \approx 1$ at 60 °C. Recently, di(diphenylmethyl) trithiocarbonate (**TTC-3**, Scheme 1c) was tested for MMA polymerization and showed moderate dispersity values ($Đ$ = 1.3–1.4), although an unusually high quantity of initiator was required to achieve only partial control over molar masses.[14] In 2021 our group reported bis(2-cyanopropan-2-yl)trithiocarbonate (**TTC-bCP**, Scheme 1c), a symmetrical trithiocarbonate with the most effective leaving group ever reported for RAFT polymerization of MMA.[15] To synthesize **TTC-bCP** we proposed an elegant route starting from 2,2′-azobis(2-methylpropionitrile) (AIBN) as a source of (2-cyanopropan-2-yl) group. Remarkably, it appeared to be extremely efficient for the preparation of all (meth)acrylic TPEs with exceptionally low dispersities for first methacrylate block and methacrylate-acrylate-methacrylate triblock copolymer ($Đ$ < 1.1).

In search of new, highly reactive symmetrical TTCs, we focused our attention on the 1-cyanocyclohex-1-yl leaving group which can be derived from V-88 initiator, namely 1,1′-azobis(cyclohexanecarbonitrile). Unexpectedly, there is very little literature on thiocarbonylthio compounds of general structure R-S(C = S)Z bearing this leaving R group. Exhaustively, it is worth mentioning works of Zard and coworkers on the synthesis of the corresponding *O*-ethyl xanthate[16] and a CSIRO patent which exemplifies the synthesis of the dithiobenzoate (Z = Ph).[17] Alternatively, the latter RAFT agent was recovered by Perrier and coworkers through radical-induced chain-end treatment of a dithiobenzoate-capped polymer with V-88 initiator.[18] Surprisingly, we found no information about the use of these compounds in RAFT polymerization. In this work, we perform a comprehensive comparative analysis between **TTC-bCP** and its counterpart, bis(1-cyanocyclohex-1-yl)trithiocarbonate (**TTC-bCCH**, **Scheme 2**) for the polymerization of St, *n*BA and MMA. For both RAFT agents, the apparent chain transfer constants were calculated for MMA polymerization and DFT calculations were carried out in order to better interpret the influence of the leaving R group on the reactivity of the RAFT agents. Furthermore, TPE properties inherent to all-(meth)acrylic ABA block copolymers produced by both TTCs were revealed by rheological characterization.

2. Results and Discussion

The synthesis of **TTC-bCCH** has been derived from our preceding work[15] by substituting 2,2′-azobis(2-methylpropionitrile) (AIBN) used for the preparation of **TTC-bCP** with 1,1′-azobis(cyclohexanecarbonitrile) (V-88, Scheme 2). The sole modification in the procedure was introduced during the synthesis of thiol **3**, which was carried out using a Kugelrohr apparatus instead of the trap-to-trap approach employed in the synthesis of 2-mercapto-2-methylpropanenitrile for **TTC-bCP**. **TTC-bCCH** has been obtained in a good yield as yellow crystals with structure confirmed by ^{1}H (Figure S13, Supporting Information), ^{13}C NMR (Figure S14, Supporting Information), and X-ray diffraction (Figure S15; Tables S5 and S6, Supporting Information).

2.1. RAFT Polymerization of St and *n*BA Mediated by TTC-bCCH

TTC-bCCH was first evaluated in the RAFT polymerization of St and *n*BA at 60 °C (**Figure 1a,b**). In the case of St polymerization (Figure 1a), it is clear that controlled M_n and low dispersities ($Đ$ < 1.07) were achieved right from the onset of polymerization. As the conversion of St increases, M_n follows a linear trend with values matching theoretical expectations. Notably,

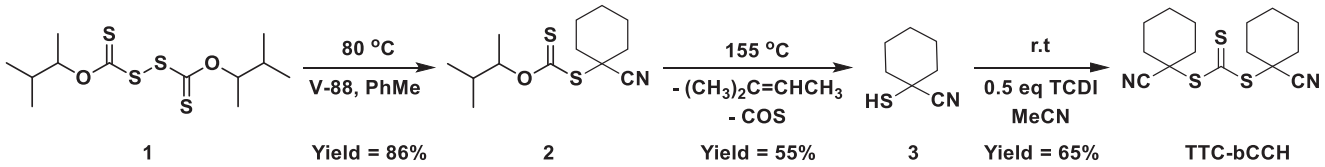

Scheme 2. Synthetic pathway for bis(1-cyanocyclohex-1-yl)trithiocarbonate **TTC-bCCH**.

$Đ$ values are remarkably low, ranging between 1.03 and 1.04 within the 33–88% conversion range (Table S1, entry 3–5, Supporting Information). Very similar results have been obtained for the RAFT polymerization of St with **TTC-bCP** (Table S2, entry 1–3, Supporting Information). This suggests that both RAFT agents exhibit swift addition-fragmentation rates, facilitating their prompt consumption. Additionally, size exclusion chromatography (SEC) analysis revealed a distinctive shoulder appearing at lower elution times, initiating at 65% conversion. This behavior can be attributed to an increased contribution of chain termination events at higher conversion. RAFT controlled polymerization of *n*BA with **TTC-bCCH** led to well-controlled M_n and low dispersities throughout polymerization (Figure 1b). Although a slightly high dispersity is observed at the beginning of the polymerization (conversion$_{(n\text{BA})}$ = 5%, $Đ$ = 1.29, Table S3, entry 1, Supporting Information), it swiftly diminishes to an excellent value of $Đ$ = 1.03 (Table S3, entry 4–6, Supporting Information). Such results confirm fast addition-fragmentation rate in polymerization of *n*BA with **TTC-bCCH**, similar to styrene polymerization. Analysis of P*n*BA using SEC-RI and -UV chromatograms reveal monomodal distributions and confirms the presence of the TTC mid-chain fragment, evident due to its strong UV absorbance (λ = 290 nm) (Figure S2, Supporting Information). Furthermore, the analysis conducted using electrospray ionization mass spectrometry (ESI-MS) on low molar mass P*n*BA (Table S3, entry 1) confirmed the incorporation of **TTC-bCCH** within the polymer structure, with P*n*BA-**TTC-bCCH** observed as the exclusive moiety across multiple populations (as depicted in Figure S4, Supporting Information). The primary population corresponds to the empirical formula $(C_7H_{12}O_2)_n$-$C_{15}H_{20}N_2S_3$, aligning with the P*n*BA-**TTC-bCCH** formula of m/z 324 $[C_{15}H_{20}N_2S_3] + 128 \times n\,[(C_7H_{12}O_2)_n] + 23$ [Na]. Minor populations represent multicharged polymers with the same formula, $(C_7H_{12}O_2)_n$-$C_{15}H_{20}N_2S$. Despite ESI-MS providing a M_n value of 2.1 kg mol^{-1} and a dispersity of 1.09, it is noteworthy that the obtained M_n value is lower compared to that obtained by SEC (8.6 kg mol^{-1}). This discrepancy can be rationalized by the higher sensitivity of the detector to lower masses, resulting in a loss of information for longer P*n*BA-**TTC-bCCH** chains.

2.2. RAFT Polymerization of MMA Mediated by TTC-bCCH

MMA polymerization in the presence of **TTC-bCCH** was conducted under exactly the same conditions as those reported for **TTC-bCP**[15] (Figure 1c). Good control over M_n is obtained at intermediate conversion of MMA (40–50%, Table S4, entry 4–5, Supporting Information) while dispersity steadily decreases from the beginning of polymerization (10% MMA conversion), which evolved from an initial value of $Đ$ = 1.43 (Table S4, entry 1, Supporting Information) to a moderate $Đ$ = 1.32 (Table S4, entry 7, Supporting Information) by the end of polymerization. SEC-RI results revealed monomodal PMMA distributions, and UV detection confirmed the presence of the TTC within the polymer chains (Figure S3, Supporting Information). ESI-MS analysis of low molar mass PMMA (Table S4, entry 1, Supporting Information) revealed the exclusive presence of PMMA-**TTC-bCCH** among the observed populations (as shown in Figure S5 in the Supporting Information). The primary population corresponds to the empirical formula $(C_5H_8O_2)_n$-$C_{15}H_{20}N_2S_3$, matching the PMMA-**TTC-bCCH** formula of m/z 244 $[C_{15}H_{20}N_2S_3] + 100 \times n\,[(C_5H_8O_2)_n] + 23$ [Na]. Minor populations display multicharged polymers with the same formula $(C_5H_8O_2)_n$- $C_{15}H_{20}N_2S_3$. Comparing the results of RAFT polymerization of MMA using **TTC-bCP**[15] and **TTC-bCCH**, a noteworthy alteration of control with the latter is clearly visible, particularly at lower conversions. This may be attributed to a lower leaving group ability for 1-cyanocyclohex-1-yl (**TTC-bCCH**) compared to 2-cyanopropan-2-yl

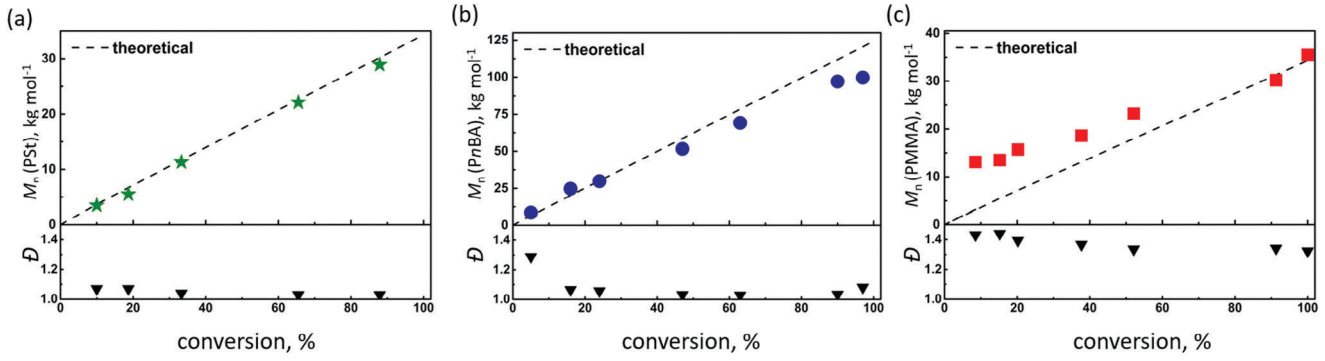

Figure 1. M_n and $Đ$ versus conversion during monomer polymerization with **TTC-bCCH** at 60 °C. SEC values determined by SEC-RI-MALS in THF. a) Styrene: $[St]_0/[\textbf{TTC-bCCH}]_0/[AIBN]_0$ = 340/1/0.1. b) *n*-Butyl acrylate: $[n\text{BA}]_0/[\textbf{TTC-bCCH}]_0/[AIBN]_0$ = 900/1/0.1. c) Methyl methacrylate: $[MMA]_0/[\textbf{TTC-bCCH}]_0/[AIBN]_0$ = 330/1/0.3 with 70 wt% MMA in acetonitrile.

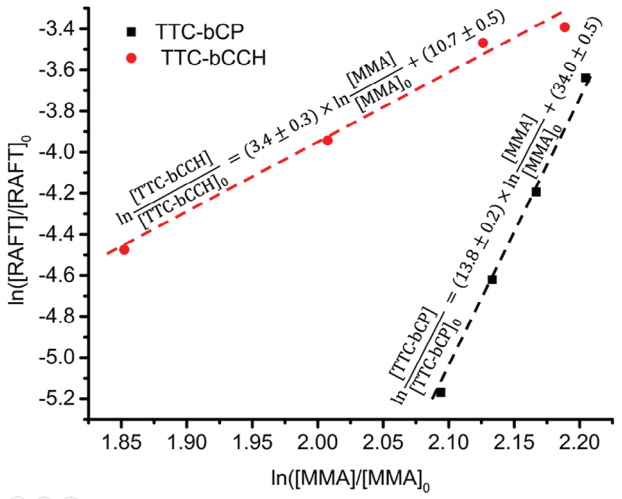

Figure 2. Double log plot of [RAFT agent] versus [MMA] for bulk polymerization at 60 °C.

(**TTC-bCP**). In order to quantify these differences, we determined the transfer constant (C_{tr}) for both RAFT agents. As conventional approaches such as the Mayo method are only valid for low C_{tr} values and hence not appropriate for most of RAFT agents, apparent transfer constants (C_{tr}^{app}, assuming $C_{-tr} = k_{-tr}/k_i$ can be neglected) were obtained by following the consumption of MMA and RAFT agent during one single RAFT polymerization.[19,20] Further details on the calculation of C_{tr}^{app} are provided in the supplementary information (ESI). C_{tr}^{app} was determined from bulk polymerizations of MMA at 60 °C. In this methodology, SEC analysis with UV detection was employed to monitor changes in TTC concentration, while MMA conversion was tracked using ^{1}H NMR spectroscopy. As illustrated on the double log plot in **Figure 2**, **TTC-bCCH** is four times less reactive than **TTC-bCCH** with $C_{tr}^{app}{}_{(TTC\text{-}bCP)} = 13.8 \pm 0.2$ and $C_{tr}^{app}{}_{(TTC\text{-}bCCH)} = 3.4 \pm 0.3$. In addition, C_{tr} for **TTC-bCCH** was measured using an alternative method based on the kinetic model developed by Müller et al.[21,22] for living polymerization systems exhibiting slow degenerative transfer (Figure S6, Supporting Information). A C_{tr} value of 5.3 ± 0.4 was determined, which is close to $C_{tr}^{app}{}_{(TTC\text{-}bCCH)}$.

Density functional theory (DFT) calculations on the addition-fragmentation chain transfer reactions of the **TTC-bCP** and **TTC-bCCH** with a unimeric methyl methacrylate derived radical are consistent with the observed lower chain transfer constant for the RAFT agent bearing 1-cyano-1-cyclohexyl substituents (**Figure 3**). While addition of the unimeric MMA radical to the initial RAFT agent has a lower barrier for the 1-cyano-1-cyclohexyl substituted species compared with the cyano-isopropyl substituted species, the barrier for the subsequent fragmentation of 1-cyano-1-cyclohexyl from the RAFT adduct radical is higher, and the overall chain transfer process is kinetically disfavored. In contrast the cyano-isopropyl derived species shows a strong kinetic preference for fragmentation of the cyano-isopropyl radical versus the MMA-derived radical, leading to efficient chain transfer. The different behavior is the result of steric effects. An examination of the noncovalent interaction analyses (Figure S18, Supporting Information) reveals that the transition states for the RAFT agent bearing 1-cyano 1-cyclohexyl substituents are understandably more hindered than the cyano-isopropyl substituted species. For the initial reaction of MMA radical to the RAFT agent this hindrance does not result in a higher barrier as the initial RAFT agent is also hindered and there is a cancellation; for fragmentation of the MMA radical steric hindrance in the transition state increases upon fragmentation giving rise to the higher barrier.

2.3. All-(meth)acrylic ABA Triblock Copolymer Synthesis and Characterization Using TTC-bCCH

Given that the **TTC-bCCH** controlled polymerization of MMA leads to a somewhat higher dispersity in comparison to **TTC-bCP**, it becomes intriguing to explore the impact of the less-defined PMMA segment on the TPE properties of the PMMA-*b*-P*n*BA-*b*-PMMA triblock copolymer. To do so, we have prepared PMMA-**TTC-bCCH** in the same polymerization conditions as those established for PMMA-**TTC-bCP** in our previous work[15] (**Table 1**, entry 1 and 3). The produced PMMA-**TTC-bCCH** had similar M_n but slightly higher dispersity ($Đ = 1.22$) compared to PMMA-**TTC-bCP** ($Đ = 1.09$). Next, an ABA block copolymer was synthesized in a convergent fashion from PMMA-**TTC-bCCH** as the hard block A (**Scheme 3**) and P*n*BA as the soft block B utilizing the same methodology as for PMMA-**TTC-bCP**.[15] **Figure 4a** illustrates the successful extension of the PMMA-**TTC-bCCH**, yielding a PMMA-*b*-P*n*BA-*b*-PMMA devoid of residual PMMA macro-CTA. This triblock exhibits a controlled M_n of 142.8 kg mol^{-1} and a low $Đ$ of 1.07 (Table 1, entry 2) closely mirroring the profile of the ABA block copolymer produced by **TTC-bCP** (M_n = 134.4 kg mol^{-1}, $Đ$ = 1.04, Figure 4b, Table 1, entry 4). Overall, both triblock copolymers have very similar profiles in differential scanning calorimetry (DSC) measurements, featuring a glass transition temperatures close to the T_g of the corresponding homopolymers (−47 and 130 °C for the soft and hard blocks respectively Table 1, entry 2). This proximity signifies effective phase separation between the constituent blocks. The elevation of the T_g of the PMMA block to 130 °C (instead of 100 °C for pure PMMA Table 1 entry 1) is aligned with the behavior observed in the **TTC-bCP** produced triblock (Table 1, entry 4), a phenomenon previously documented in certain nanophase-separated acrylic block copolymers of MMA.[23]

Thermogravimetric analysis (TGA) of the PMMA-*b*-P*n*BA-*b*-PMMA triblock revealed its excellent stability, with less than 5% weight loss observed at 280 °C in air and at 350 °C under inert conditions (Figure S8, Supporting Information).

The impact of dispersity on the thermomechanical properties was evaluated by rheology measurements over a temperature ramp from 20 to 180 °C. Figure S16 (Supporting Information) displays the temperature dependence of G' and G'' of PMMA-P*n*BA-PMMA triblock copolymers with similar composition made from both **TTC-bCCH** and **TTC-bCP** RAFT agents (Table 1, entry 2 and 4, respectively). The materials showed a typical storage modulus (G') for elastomeric material within the range of 1 MPa. Although a similar modulus was obtained at 20 °C for both materials, a different temperature dependence was noticed for the PMMA-P*n*BA-PMMA triblock with larger dispersity of the PMMA blocks, with a progressive drop of G'

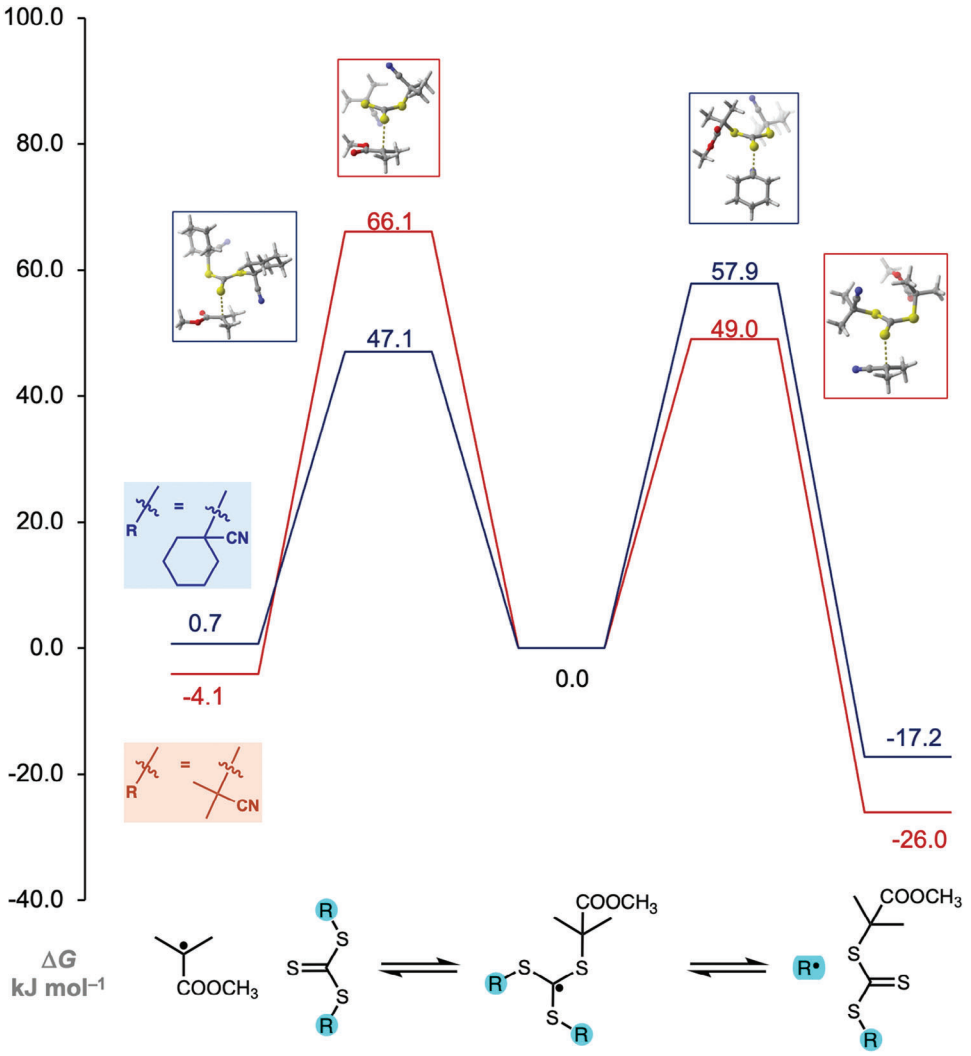

Figure 3. Gibbs free energy profiles (60 °C, kJ mol^{-1}) of the addition-fragmentation processes studied at the wB97XD/def2-TZVPP//wB97XD/6-31g(d) level of theory using SMD to model the ethyl acetate solvent. The red line refers to the reaction of a RAFT agent (S = C(SR)$_2$) bearing cyanoisopropyl R-groups with a unimeric model of a methyl methacrylate propagating radical to form an intermediate radical that then undergoes β-scission to yield the cyanoisopropyl R• radical. The blue line refers to the corresponding reaction of a RAFT agent (S = C(SR)$_2$) bearing 1-cyanocyclohex-1-yl R-groups. All energies are quoted relative to their respective intermediate radicals.

Table 1. PMMA-*b*-P*n*BA-*b*-PMMA triblock copolymer synthesis using **TTC-bCP** or **TTC-bCCH** as chain transfer agents.

Entry	RAFT agent	Prepared polymer	Time [h]	Conv. [%][a]	$M_{n\,th}$ [kg mol^{-1}][b]	$M_{n\,SEC}$ [kg mol^{-1}][c]	$Đ$[d]	T_g [°C]
1	**TTC-bCCH**	PMMA-**TTC-bCCH**[d]	24	98.2	32.9	38.7	1.22	100
2	PMMA-**TTC-bCCH**	PMMA-P*n*BA-PMMA[e]	12.3	91	146.5	19.3-104.1-19.3 (142.8)[f]	1.07	130 (−47)[g]
3[h]	**TTC-bCP**	PMMA-**TTC-bCP**[d]	40	99.9	32.8	34.8	1.09	n.d.
4[h]	PMMA-**TTC-bCP**	PMMA-P*n*BA-PMMA[e]	13.5	88.6	141.1	17.4-99.6-17.4 (134.4)[f]	1.04	124 (−57)[g]

[a] Conversions determined by ^{1}H NMR; [b] $M_{n(th)} = ([M]_0/[RAFT]_0) \times \text{conversion}(M) \times M_W(M) + M_W(\textbf{CTA})$; [c] Determined by SEC-RI-MALS in THF; [d] Polymerization has been conducted at 60 °C with 70 wt% MMA in acetonitrile with a ratio of $[MMA]_0/[RAFT]_0/[AIBN]_0 = 330/1/0.3$; [e] Polymerization of *n*BA has been conducted at 60 °C in bulk with a ratio of $[nBA]_0/[RAFT]_0/[AIBN]_0 = 930/1/0.1$; [f] M_n for triblock copolymers determined by SEC-RI-MALS are given in parentheses, while values for each blocks are calculated based on M_n of the PMMA-TTC used for chain extension such as A–B–A, where A = M_n(PMMA)/2 and B = M_n(SEC) − M_n(PMMA); [g] In parentheses, T_g value of the soft P*n*BA block is shown; [h] Taken from ref. [15].

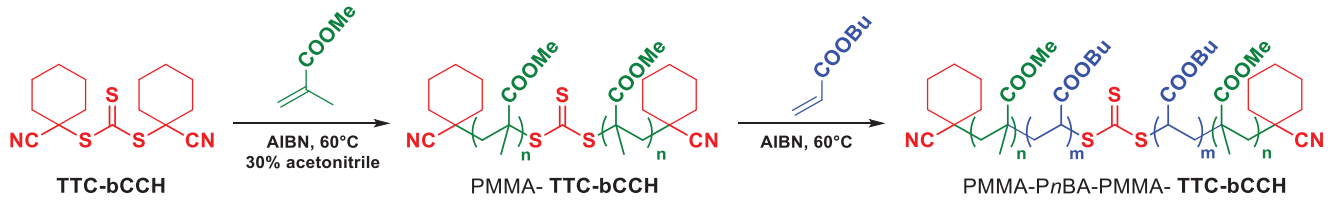

Scheme 3. PMMA-P*n*BA-PMMA triblock copolymer synthesis using **TTC-bCCH** as a chain transfer agent.

with increasing temperature. This difference can be explained by various factors, including an effect of dispersity on the phase diagram,[24] with possible modifications of phase boundaries.[25] Additionally, the presence of low molecular weight chains, either not integrated or only partially integrated into rigid domains, are known to contribute to a decrease in polymer stiffness and yield stress.[26] Given the complexity of the system and the various parameters to consider, the impact of dispersity on phase diagram morphologies and mechanical properties will be studied in a dedicated publication.

3. Conclusion

This study expands the range of available leaving groups for RAFT agents with novel bis(1-cyanocyclohex-1-yl)trithiocarbonate **TTC-bCCH**, which is an effective RAFT agent for St, *n*BA and MMA. Based on the determination of transfer constants to RAFT agents and DFT calculations, it has been established that the 1-cyanocyclohex-1-yl of **TTC-bCCH** is a less good leaving group than 2-cyanopropan-2-yl in **TTC-bCP**. However, **TTC-bCCH** is still much more reactive than previously reported **TTC-1**, **TTC-2**, and **TTC-3**. Typical storage moduli (G') for elastomers were obtained for ABA triblock copolymers made with **TTC-bCCH**. Lower stability towards temperature was revealed, suggesting differences in structuration possibly due to the presence of lower molecular weight PMMA blocks. Further investigations will be needed to better understand this effect.

4. Experimental Section

Materials and Methods: The following chemicals were used as received, 3-methylbutan-2-ol (97%, Sigma-Aldrich), KOH (≥98%, Sigma-Aldrich), CS_2 (97%, Sigma-Aldrich), iodine (99.9%, Sigma-Aldrich), potassium iodide (97%, Sigma-Aldrich), sodium thiosulfate (97%, Sigma-Aldrich), 1,1′-thiocarbonyldiimidazole (TCDI, 99%, Sigma-Aldrich), 1,1′-azobis(cyclohexanecarbonitrile) (V-88, 98%, Sigma-Aldrich). The following chemicals were purified before use: 2,2′-azobis(2-methylproprionitrile) (AIBN, 98%, Sigma-Aldrich) was recrystallized from methanol and dried under vacuum. Styrene (St, ≥99%, Sigma-Aldrich), *n*-butyl acrylate (*n*BA, ≥99%, Sigma-Aldrich), and methyl methacrylate (MMA, >99%, Sigma-Aldrich) were purified by passing through neutral Al_2O_3. **TTC-bCP** and di(3-methylbutan-2-yl) dixanthogen **1** were synthesized as was previously reported.[15]

The following solvents were used as received: petroleum ether (Sigma-Aldrich, HPLC grade), *n*-pentane (Sigma-Aldrich, HPLC grade), ethyl acetate (EtOAc, Sigma-Aldrich, HPLC grade), and cyclohexane (Sigma-Aldrich, HPLC grade). THF (Sigma-Aldrich, HPLC grade), toluene (Sigma-Aldrich, HPLC grade), and acetonitrile (MeCN, Acros, HPLC grade) were dried using a solvent purifier (MBRAUN SP5).

Nuclear magnetic resonance (NMR) spectra (^{1}H, ^{13}C) were recorded at 25 °C on a Bruker Avance 300 MHz instrument. J is reported to ± 0.5 Hz. The resonance multiplicities are described as s (singlet), d (doublet), t (triplet), q (quartet), or m (multiplet). ^{13}C NMR and J-mod ^{13}C NMR spectra were recorded at 75.47 MHz. Chemical shifts δ are reported in parts per million (ppm) and are referenced to the residual solvent peak ($CDCl_3$: H = 7.26 ppm and C = 77.16 ppm).

Size-exclusion chromatography (SEC) analyses in THF was performed on a system composed of an Agilent Technologies guard column (PLGel20 µm, 50 × 7.5 mm) and a set of three Shodex columns (KF-805 + KF-804 + KF-802.5). Detections were conducted using a Wyatt Optilab rEX refractive index detector, a Varian ProStar 325 UV detector (dual wavelength analysis) and a Wyatt MiniDawn TREOS multi-angle light scattering (MALS) detector. Analyses were performed at 35 °C and a flow rate of 1.0 mL min^{-1}. The following refractive index increment (dn/dc) values were used for the determination of average molar masses: $(dn/dc)_{PMMA} = 0.085$[1] and $(dn/dc)_{PnBA} = 0.067$ and $(dn/dc)_{St} = 0.185$.[2] The column system was calibrated with PMMA standards (ranging from 960 to 265 300 g mol^{-1}). Number-average (M_n) and weight-average (M_w) molar masses were evaluated using Waters Empower software. SEC-RI traces were converted from the elution volume scale into a molar mass

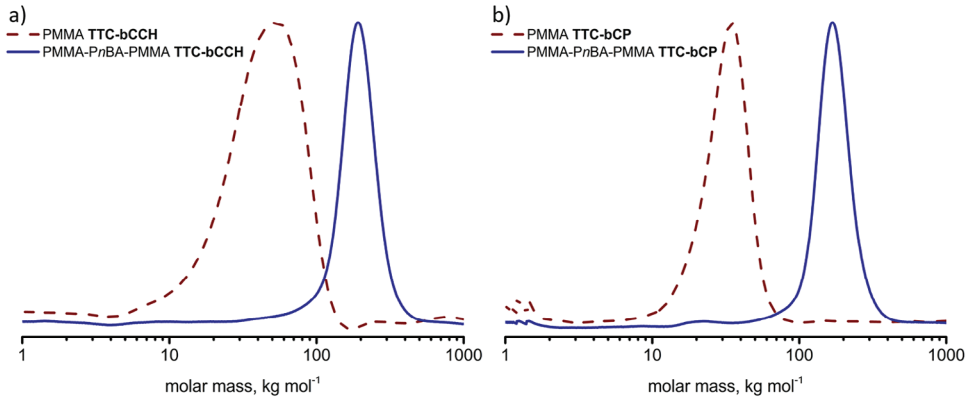

Figure 4. SEC traces of PMMA-**TTC** and PMMA-P*n*BA-PMMA triblock copolymers prepared with a) **TTC-bCCH** or b) **TTC-bCP**.

scale (log scale) using a PMMA calibration curve, using the following equation: log(Molar Mass) = 9.71611 – 0.288372 t + 0.00267245 t^2. This equation was obtained from SEC-RI calibration dataset using Wyatt Astra software.

Rheology experiments were performed on an Anton Paar MCR 302. The experiments were performed in parallel plate geometry using 8 mm sample disks. For temperature ramp experiments an oscillating frequency of 1 Hz and a strain of 1% was applied and G', G'', and tanδ was followed. The applied stress of 1% was comprised in the linear viscoelastic region at the measured temperatures. Sample preparation: 300 mg of a poly(methyl methacrylate)-*b*-poly(*n*-butyl acrylate)-*b*-poly(methyl methacrylate) triblock copolymer was pressed in the rheometer at 200 °C for 15 min. Then, the temperature was cooled down to 20 °C, and subsequently raised at a rate of 3 °C min^{-1}.

ESI-MS Analysis was carried out with 1,8-dihydroxy-9(10*H*)-anthracenone (Dithranol) as the matrix and NaI salt as the cationizing agent. ESI-TOF mass spectra were acquired with a Xevo G2 QTOF mass spectrometer (Waters) in electrospray ionization in positive mode. A sample of polymer was dissolved in chloroform, diluted at 1/10 with acetonitrile and then an acetone solution of NaI (10 mg mL^{-1}) was added. On the Xevo G2 QTOF, the injection was made in Flow Injection Analysis (FIA). The source temperature and desolvation temperature were 110 and 350 °C, respectively, and the cone voltage was optimized at 50 V. The acquisition software was Masslynx (Waters) and the spectra were processed by using Masslynx and Polymerix 3.0 (Sierra Analytics).

The glass transition temperature (T_g) of the polymers was measured by differential scanning calorimetry (DSC) using Mettler Toledo STARe DSC in nitrogen atmosphere using aluminum crucibles of 40 µL at heating rates of 10 °C min^{-1}. Samples in 10–15 mg portions were used in the analysis. All T_g values were obtained from the second scan to remove the thermal history of the samples.

X-ray diffraction—Crystallographic data were collected at 193(2) K on a Bruker-AXS D8-Venture using MoK_α radiation (λ = 0.71073 Å) and equipped with a PHOTON III detector. Phi- and omega-scans were used. Empirical absorption correction was employed.[3] The structures were solved using an intrinsic phasing method (SHELXT),[4] and refined using the least-squares method on F^2.[5] All non-H atoms were refined with anisotropic displacement parameters. Hydrogen atoms were refined isotropically at calculated positions using a riding model.

Thermogravimetric analysis—TGA analyses were conducted on a TGA/DSC3 + Mettler with a temperature ramp of 10 °C min^{-1} under N_2 (50 mL min^{-1}).

Determination of the chain transfer constant to RAFT agent—Mayo method[27] may be used to estimate C_{tr} provided that the evolution of chain transfer agent and monomer concentrations are negligible. As it is no longer valid for highly reactive RAFT systems, another method described below based on kinetic equations can be applied. The rate of consumption of RAFT agent X (Equation 1) and Monomer M (Equation 2) are expressed as follows

$$-\frac{d[X]}{dt} = k_{tr,X}[P\bullet][X] - k_{-tr,X}[R\bullet][PnX] \quad (1)$$

$$-\frac{d[M]}{dt} = k_p[P\bullet][M] + k_r[R\bullet][M] \quad (2)$$

Where k_{tr} is the rate constant of chain transfer to RAFT agent, k_{-tr} is the rate constant of reverse chain transfer, k_p is the rate constant of propagation and k_r is the rate constant of reinitiation.

In the case of reversible chain transfer, the rate of consumption of the transfer agent depends on two transfer constants ($C_{tr} = k_{tr}/k_p$ and $C_{-tr} = k_{-tr}/k_p$), which describe the reactivity of the propagating radical (Pn•), and the expelled radical (R•) respectively, therefore the Equations (1) and (2) could be transformed to

$$\frac{d[X]}{d[M]} = C_{tr,X}\frac{[X]}{[M] + C_{tr,X}[X] + C_{-tr,X}[PnX]} \quad (3)$$

If the rate of the reverse reaction between R• and Macro-RAFT agent PnX (4) is negligible, therefore rendering negligible C_{-tr}, this expression (Equation (3)) simplifies to Equations (4) and (5)

$$\frac{d[X]}{d[M]} \approx C_{tr,X}\frac{[X]}{[M]} \quad (4)$$

$$\ln\frac{[X]}{[X]_0} \approx C_{tr,X}\ln\frac{[M]}{[M]_0} \quad (5)$$

Given these considerations, the slope of a plot of $\ln([M]/[M]_0)$ versus $\ln([X]/[X]_0)$ yields the apparent chain transfer constant C_{tr}^{app}. The monitoring of a single polymerization is sufficient to obtain reliable C_{tr}^{app} estimate.

DFT Computational methods—The geometries of all structures of interest along the addition-fragmentation processes under consideration were optimized at the SMD[28]-(ethyl acetate)-wB97XD[29]/6-31g(d)[30–33] level of theory. Harmonic frequency calculations were performed at the same level of theory, confirming that all optimized equilibrium structures have all real frequencies while all optimized transition structures have one imaginary frequency pertaining to the motion along the reaction coordinate of interest. Intrinsic reaction coordinate (IRC) calculations[34] were further performed on all transition structures to confirm connectivity to the correct reactants and products. Conformational searches with resolutions of typically 120° around sp^3–sp^3 bonds and 180° around sp^2–sp^3 bonds were performed at the SMD[28]-(ethyl acetate)-wB97XD[29]/6-31g(d)[30–33] level of theory on all flexible structures along the addition-fragmentation processes to obtain global minimum conformations. The accuracy of electronic energies was subsequently improved at the SMD[28]-(ethyl acetate)-wB97XD[29]/def2-TZVPP[35] level of theory and the frequencies obtained at the SMD[28]-(ethyl acetate)-wB97XD[29]/6-31g(d)[30–33] level of theory were used to calculate zero-point vibrational energies, thermal corrections to the enthalpy, and entropic corrections within the harmonic oscillator/rigid rotor approximation. Solution phase Gibbs free energies were calculated using the "direct method" of Truhlar and coworkers,[36] which applies ideal gas partition functions to solution-phase geometries and frequencies. A correction for the change of state from 1 atm to 1 M was further included.[37] All geometry optimizations, frequency, and single point energy calculations were carried out using the Gaussian16[38] program package. 3D visualizations were generated with CYLview.[39] Multiwfn[40] and VMD 1.9.4[41] were used to perform Noncovalent interactions (NCI) analyses[42] and generate NCI plots and spin density plots.

Experimental procedure to estimate C_{tr}^{app}—AIBN (0.3 equiv), RAFT agent (1 equiv), and MMA (220 equiv) were combined. The resulting stock solution was then divided, with a portion being utilized for SEC analysis to determine an initial estimate of TTC conversion (t_0). The remaining stock solution was divided further and transferred to glass ampoules. The glass ampoules were flame-sealed following degassing through three freeze–pump–thaw cycles. These sealed ampoules were then immersed in a 60 °C oil bath for 0.5, 1, 2, and 3 h for polymerization. The polymerization reaction was terminated by rapid cooling. Upon opening the ampoules, three small aliquots of the solution were promptly transferred to separate NMR tubes for the analysis of MMA conversion. The other portion of the solution was transferred to vials for 3 repeated SEC-UV analysis (at 290 nm).

Typical polymerization method—AIBN, TTC, and the monomer were dissolved in the suitable solvent, if required. The resulting solution was then transferred into glass ampoules, which were sealed with flames after degassing through three freeze–pump–thaw cycles. Subsequently, the sealed ampoules were immersed in an oil bath at 60 °C. The polymerization process was halted by rapid cooling. Upon opening the ampoules, the solutions were promptly transferred into NMR tubes for conversion analysis. The volatile components were removed under vacuum, and the remaining solution was used to prepare samples for SEC analysis.

S-(2-cyanocyclohexan-2-yl) O-(3-methylbutan-2-yl) xanthate **2**. Di(3-methylbutan-2-yl) dixanthogen **1** (11.8 mmol, 3.85 g) and V-88 (16 mmol, 3.91 g) were dissolved in dry toluene. The solution was degassed and purged with Ar. The resulting solution was then placed in an oil bath at 104 °C for 2.5 h. If any starting material remains (NMR analysis is

required), an additional portion of V-40 (8 mmol, 1.95 g) is added after 2 h, followed by an additional 5-h incubation in the oil bath. Purification was performed using column chromatography, with a *n*-pentane/diethyl ether mixture as the eluent in a 95:5 ratio. The final product was obtained as a yellow oil. 2.93 g (86%).

^{1}H NMR (300 MHz, $CDCl_3$, δ): 5.62 (q, 1H, CH-CH(CH_3)-O); 2.31 (m, 4H, CH_2-CCH_2); 2.17 (m, 1H, CH-CH(CH_3)$_2$); 2.07 (m, 1H, CH-CH(CH_3)$_2$); 1.72 (m, 6H, CH_2-CH_2-CH_2-CH_2-CH_2); 1.39 (d, 3H, CH-CH(CH_3)O); 1.04 (dd, 6H, CH(CH_3)$_2$). ^{13}C NMR (75 MHz, $CDCl_3$, δ): 207.88 (O(C = S)S); 119.85 (CN); 87.34 (CH-CH(CH_3)-O); 47.03 (S-C(CH_2)$_5$-CN); 35.41 (S-C(CH2)$_5$CN); 32.41 (CH-CH(CH_3)-O); 24.69-22.87 (CH_2-(CH_2)$_3$-CH_2); 18.36-17.83 (CH(CH_3)$_2$); 15.48 (CH(CH_3)-O).

1-mercaptocyclohexane-1-carbonitrile ***3***. A Chugaev elimination was conducted by heating at 155 °C for 2 h. Specifically, 3.49 g (12.8 mmol) of S-(2-cyanocyclohexan-2-yl) O-(3-methylbutan-2-yl) carbonodithioate **2** was subjected to the reaction using a short-path distillation apparatus, specifically a Kugelrohr system. The resulting product was obtained as a strongly aromatic, colorless liquid, with a yield of 1.00 g (55%).

^{1}H NMR (300 MHz, $CDCl_3$, δ): 5.71 (s, 1H, SH); 2.10 (m, 2H, CH_2-C-CH_2); 1.58 (m, 7H, (CH_2-CH_2-CH_2-CH_2-CH_2); 1.20 (q, 1H, CH_2-CH_2-CH_2-CH_2-CH_2). ^{13}C NMR (75 MHz, $CDCl_3$, δ): 122.11 (CN); 39.70 (HS-C(CH_2)$_5$CN); 35.41 (S-C(CH_2)$_5$-CN); 32.41 (CH-CH(CH_3)-O); 24.27-23.49 (CH_2-(CH_2)$_3$-CH_2).

Bis(1-cyanocyclohexyl) carbonotrithioate ***TTC-bCCH***. A solution of dry acetonitrile (10 mL) and thiocarbonyldiimidazole (TCDI, 0.39 g, 2.22 mmol) was prepared. To this solution, a solution of (1-mercaptocyclohexyl) methanenitrile (0.63 g, 4.45 mmol) in dry acetonitrile (10 mL) was added dropwise under an argon atmosphere. The reaction mixture was thoroughly mixed and allowed to stir for one hour under argon. During this time, a change in color was observed, transitioning from yellow to a vibrant orange hue. Subsequently, the reaction solvent was removed under reduced pressure. The resulting product was obtained through column filtration, utilizing a mixture of 50% ethyl acetate and 50% cyclohexane as the eluent. The purity of the compound after column purification was ≈80–90%, with a disulfide impurity content of 10%. The yield achieved was 65% (0.269 g). Recrystallization in *n*-pentane of the product was performed to remove impurities. ^{1}H NMR (300 MHz, $CDCl_3$, δ): 2.55 (q, 8H, CH_2-C-CH_2); 1.77 (m, 8H, (CH_2-CH_2-CH_2-CH_2-CH_2); 1.40 (m, 4H, (CH_2-CH_2-CH_2-CH_2-CH_2). ^{13}C NMR (75 MHz, $CDCl_3$, δ): 209.85 (S-C(= S)S); 118.48 (CN); 49.57 (S-C(CH_2)$_5$-CN); 35.39 (S-C(CH_2)$_2$CN); 24.80 (CH_2-CH_2-CH_2-CH_2-CH_2); 22.84 (CH_2-CH_2-CH_2-CH_2-CH_2).

[CCDC 2 352 086 contains the supplementary crystallographic data for this paper. These data can be obtained free of charge from The Cambridge Crystallographic Data Centre via www.ccdc.cam.ac.uk/data_request/cif.]

Supporting Information

Supporting Information is available from the Wiley Online Library or from the author.

Acknowledgements

The authors thank Pascale Laborie, Institut de Chimie de Toulouse ICT-UAR 599, for her technical assistance with SEC analyses and Lucie Perquis, Assistante Ingénieur CNRS, for her valuable help with DSC analysis. M.L.C. acknowledges support from the Australian Research Council (CE230100021), and generous allocations of supercomputing time on the National Facility of the Australian National Computational Infrastructure and Flinders Deepthought.

Conflict of Interest

The authors declare no conflict of interest.

Data Availability Statement

The data that support the findings of this study are available from the corresponding author upon reasonable request.

Keywords

DFT calculations, kinetics, RAFT, triblock copolymers, trithiocarbonate

Received: May 7, 2024
Revised: May 29, 2024
Published online: June 18, 2024

[1] R. T. A. Mayadunne, E. Rizzardo, J. Chiefari, J. Krstina, G. Moad, A. Postma, S. H. Thang, *Macromolecules* **2000**, *33*, 243.
[2] G. Moad, E. Rizzardo, S. H. Thang, *Aust. J. Chem.* **2012**, *65*, 985.
[3] "Buy Chemicals Online @Catalogue," https://www.boronmolecular.com/raft-agents/ (accessed: April 2024).
[4] M. Destarac, *Polym. Chem.* **2018**, *9*, 4947.
[5] W. Wang, W. Lu, A. Goodwin, H. Wang, P. Yin, N.-G. Kang, K. Hong, J. W. Mays, *Prog. Polym. Sci.* **2019**, *95*, 1.
[6] K. Kunal, A. Mamtani, "Thermoplastic Elastomers Market Size & Share | Statistics –2023," https://www.gminsights.com/industry-analysis/thermoplastic-elastomers-tpe-market-report (accessed: April 2024).
[7] F. Ariura, *J. Adhes. Soc. Jpn.* **2013**, *49*, 336.
[8] K. Hamada, Y. Morishita, T. Kurihara, K. Ishiura, in *Anionic Polymerization: Principles, Practice, Strength, Consequences and Applications* (Eds.: N. Hadjichristidis, A. Hirao), Springer Japan, Tokyo **2015**, p. 1011.
[9] J.-M. Boutillier, J.-P. Disson, M. Havel, R. Inoubli, S. Magnet, C. Laurichesse, D. Lebouvier, "Self-Assembling Acrylic Block Copolymers for Enhanced Adhesives Properties," https://www.adhesivesmag.com/articles/91909-self-assembling-acrylic-block-copolymers-for-enhanced-adhesives-properties (accessed: April 2024).
[10] E. V. Chernikova, P. S. Terpugova, A. A. Baskakov, A. V. Plutalova, E. S. Garina, E. V. Sivtsov, *Polym. Sci. Ser. B* **2010**, *52*, 119.
[11] J. T. Lai, D. Filla, R. Shea, *Macromolecules* **2002**, *35*, 6754.
[12] J. Ma, H. Zhang, *Macromol. Res.* **2015**, *23*, 67.
[13] R. L. Atkinson, O. R. Monaghan, M. T. Elsmore, P. D. Topham, D. T. W. Toolan, M. J. Derry, V. Taresco, R. A. Stockman, D. S. A. D. Focatiis, D. J. Irvine, S. M. Howdle, *Polym. Chem.* **2021**, *12*, 3177.
[14] A. L. Robles Grana, H. Maldonado-Textle, J. R. Torres-Lubián, C. St Thomas, R. Díaz de León, J. L. Olivares-Romero, L. Valencia, F. J. Enríquez-Medrano, *Molecules* **2021**, *26*, 4618.
[15] O. Ivanchenko, M. Odnoroh, S. Mallet-Ladeira, M. Guerre, S. Mazières, M. Destarac, *J. Am. Chem. Soc.* **2021**, *143*, 20585.
[16] G. Bouhadir, N. Legrand, B. Quiclet-Sire, S. Z. Zard, *Tetrahedron Lett.* **1999**, *40*, 277.
[17] E. Rizzardo, S. H. Thang, G. Moad, T. P. Le, Synthesis of dithioester chain transfer agents and use of bis(thioacyl) disulfides or dithioesters as chain transfer agents (Commonwealth Scientific Research and Industrial Organization and E.I. Dupont de Nemours and Company), PCT WO99/05099, **1999**.
[18] S. Perrier, P. Takolpuckdee, C. A. Mars, *Macromolecules* **2005**, *38*, 2033.
[19] Y. K. Chong, J. Krstina, T. P. T. Le, G. Moad, A. Postma, E. Rizzardo, S. H. Thang, *Macromolecules* **2003**, *36*, 2256.
[20] M. Destarac, *Polym. Rev.* **2011**, *51*, 163.
[21] A. H. Müller, D. Yan, G. Litvinenko, R. Zhuang, H. Dong, *Macromolecules* **1995**, *28*, 7335.
[22] G. Litvinenko, A. H. Müller, *Macromolecules* **1997**, *30*, 1253.

[23] D. J. Haloi, S. Ata, N. K. Singha, D. Jehnichen, B. Voit, *ACS Appl. Mater. Interfaces* **2012**, *4*, 4200.
[24] A.-V. Ruzette, S. Tencé-Girault, L. Leibler, F. Chauvin, D. Bertin, O. Guerret, P. Gérard, *Macromolecules* **2006**, *39*, 5804.
[25] S. I. Rosenbloom, B. P. Fors, *Macromolecules* **2020**, *53*, 7479.
[26] S. I. Rosenbloom, D. T. Gentekos, M. N. Silberstein, B. P. Fors, *Chem. Sci.* **2020**, *11*, 1361.
[27] F. R. Mayo, *J. Am. Chem. Soc.* **1943**, *65*, 2324.
[28] A. V. Marenich, C. J. Cramer, D. G. Truhlar, *J. Phys. Chem. B* **2009**, *113*, 6378.
[29] J.-D. Chai, M. Head-Gordon, *Phys. Chem. Chem. Phys.* **2008**, *10*, 6615.
[30] W. J. Hehre, R. Ditchfield, J. A. Pople, *J. Chem. Phys.* **1972**, *56*, 2257.
[31] P. C. Hariharan, J. A. Pople, *Theoret. Chim. Acta* **1973**, *28*, 213.
[32] M. M. Francl, W. J. Pietro, W. J. Hehre, J. S. Binkley, M. S. Gordon, D. J. DeFrees, J. A. Pople, *J. Chem. Phys.* **1982**, *77*, 3654.
[33] M. S. Gordon, J. S. Binkley, J. A. Pople, W. J. Pietro, W. J. Hehre, *J. Am. Chem. Soc.* **1982**, *104*, 2797.
[34] C. Gonzalez, H. B. Schlegel, *J. Chem. Phys.* **1989**, *90*, 2154.
[35] F. Weigend, R. Ahlrichs, *Phys. Chem. Chem. Phys.* **2005**, *7*, 3297.
[36] R. F. Ribeiro, A. V. Marenich, C. J. Cramer, D. G. Truhlar, *J. Phys. Chem. B* **2011**, *115*, 14556.
[37] J. Ho, A. Klamt, M. L. Coote, *J. Phys. Chem. A* **2010**, *114*, 13442.
[38] M. J. Frisch, G. W. Trucks, H. B. Schlegel, G. E. Scuseria, M. A. Robb, J. R. Cheeseman, G. Scalmani, V. Barone, G. A. Petersson, H. Nakatsuji, X. Li, M. Caricato, A. V. Marenich, J. Bloino, B. G. Janesko, R. Gomperts, B. Mennucci, H. P. Hratchian, J. V. Ortiz, A. F. Izmaylov, J. L. Sonnenberg, F. D. Williams, F. Lipparini, F. Egidi, J. Goings, B. Peng, A. Petrone, T. Henderson, D. Ranasinghe, V. G. Zakrzewski, et al., in *Gaussian 16 Rev. C.01*, *Vol*. Wallingford, CT, **2016**.
[39] CYLview20; Legault, C. Y., Université de Sherbrooke, **2020**, http://www.cylview.org.
[40] T. Lu, F. Chen, *J. Comput. Chem.* **2012**, *33*, 580.
[41] W. Humphrey, A. Dalke, K. Schulten, *J. Mol. Graphics* **1996**, *14*, 33.
[42] E. R. Johnson, S. Keinan, P. Mori-Sánchez, J. Contreras-García, A. J. Cohen, W. Yang, *J. Am. Chem. Soc.* **2010**, *132*, 6498.